

MODELLING AND NUMERICAL ANALYSIS OF NONLINEAR DYNAMIC INVERSION BASED CONTROLLER FOR AN AIRCRAFT MODEL

AL-TAYYAR, H. A.

*College of Engineering, University of Mosul, Mosul, Iraq.
e-mail: huda.aqeel[at]uomosul.edu.iq*

(Received 29th September 2022; accepted 10th November 2022)

Abstract. Aircraft systems are nonlinear in nature and this will force the designer to use many linear controllers, thereafter gain scheduling them depending on the aircraft's operating system. The dynamic inversion controller is characterized by its non-linear handling of aircraft, so it is appropriate for a variety of operating conditions such as sharp angles of launch, swoop, and high speed. In this paper a design of a nonlinear dynamic inversion controller has analyzed for aircraft dynamics. The performance verification of this controller has employed by MATLAB toolbox as simulation systems. A discussion of a dynamic inversion model, which produces a controller with two loops; the inner feedback as linearization loop and the second loop as outer tracking, has been presented. One of the most important features of this method is that it makes the feedback closed simultaneously, which enhances the specifications of the controller and reaches the desired results. The results have shown when increasing in the gain, the time needed to enter steady state and stability dynamics will be less. On the other hand the amplitude of un-stability and curve distortion in the beginning dynamics curve will be stronger as gain increased. There is a need of tradeoff between two cases to get reasonable performance of aircraft control model.

Keywords: *aircraft control model, controlled variables, linearization loop, nonlinear dynamic inversion controller, proportional controller gain, stability*

Introduction

Given the importance of the control system in the movement of aircrafts during their flights, the controller is the heart of the aircraft's dynamic system. In order to reach an acceptable control, it is necessary to achieve matching the shape of the input and output signals (Almalah and Al-Tayyar, 2020). As the operating points extend, the gain scheduling used in linear control techniques will be cumbersome and useless. To overcome the problem of linear control techniques, non-linear techniques are usually applied as a suitable and effective alternative (Laxman et al., 2020). The best way to deal with nonlinear model is to use a nonlinear controller based mainly on a linearization feedback scheme. Thus, the issue of gain scheduling will be overcome. Depending on this method, the feedback loops have closed simultaneously, which results in the desired performance of the system. This is in contrast to classic techniques that depend on trial and error to successfully close the loop and get gain individually (Stevens et al., 2015). The NDI method is widely used in highly flexible aviation applications where an exact model of the aircraft is required in addition to specific system inputs (Bhardwaj et al., 2019). It can be list the important advantages of choosing this method as follows (Lombaerts et al., 2020): (1) complete isolation between steering commands, which in turn will facilitate the steering task effectively; (2) to achieve the absence of the need for scheduling the gain, the controller will be dependent and independent within the same model; and (3) the total controller includes references signals for comparison, command formation, and other functions.

In Di Francesco and Mattei (2016), the control system has installed in the aircraft based on incremental nonlinear dynamic inversion (INDI). The principle of time separation has adopted and the controller has divided into two circuits: the external control for slow movement and the internal control for the faster movement. The controller has been tested on hover and forward-flight dynamics and trying to access commonality operating points. The incremental method in nonlinear dynamic inversion control is useful in the applications presented in the two papers by Sieberling et al. (2010) and Smeur et al. (2018), because this method does not require complex modeling as well as it is computationally efficient. This method studies issues related to the stability and performance of the system, such as the analytical stability analysis, as far as the gain of the controller is concerned, and simulation using the real-time time delay algorithm to get rid of the oscillator behavior of the system (van't Veld et al., 2018). In fact INDI needs many analyzes in addition to the problem of unsatisfactory stability, so the paper (Wang et al., 2019) has used the INDI controller but without the concept of time separation. The closed loop control system has analyzed using Lypunov's method and nonlinear system disturbance theory. In addition, it can also be used to analyzing the power of the closed loop system against jammers.

Another well-known issue in NDI is saturation of actuator. The paper (Matamoros and de Vissery, 2018) has used the Incremental Nonlinear Control Allocation method to overcome this problem for tailless airplanes with robust effectors. However, when the aircraft's system and data are inaccurate, it will cause the controller's performance to degrade and the carrier landing failure. So in the paper (Lu and Liu, 2019) the design of the L1 adaptive controller taking into consideration matched and unmatched model suspicions which shows the effect of the controller depending on nonlinear dynamic inversion (NDI). The NDI designed in vehicles has discussed in the paper (Lombaerts et al., 2020). Due to the specifications of this method, it has been applied in VTOL vehicles and under various conditions.

Materials and Methods

The development of communications and air traffic around the world has increased the interest of researchers in this field to improve the performance of the system, track the movement of aircraft and control their path (Al-Tayyar and Almalah, 2020). It is necessary to discuss a dynamic inversion model, which produces a controller with two loops; the inner feedback as linearization loop and the second loop as outer tracking.

Choosing controlled variables

To ensure the success of dynamic inversion, the control variables must be chosen to the output of the system, $y(t)$. The importance of choosing the control variables lies in maintaining the stability of the so-called zero dynamics. This is done by checking the poles of the output matrix, C . If the poles p is unstable, a new output matrix must be chosen until a suitable matrix C is found, then p will be chosen as the error dynamic (Stevens et al., 2015). The airplane dynamics can be converted into space control form, so the outer loop of dynamics can be written in state space equations as:

$$\dot{x}(t) = f(x, t) + G(x, t) U(t) \quad \text{Eq. (1)}$$

$$y(t) = C x(t) \quad \text{Eq. (2)}$$

where, C_o is an output measurement matrix. Actually, The outputs to be controlled in aircraft have usually selected as:

$$\text{Pitch axis controlled variable} = q + N_z p / V_{CO} \quad \text{Eq. (3)}$$

$$\text{roll axis controlled variable} = p + \alpha r \quad \text{Eq. (4)}$$

$$\text{yaw axis controlled variable} = r - \alpha p - (g \sin \theta \cos \theta) / V + k \beta \quad \text{Eq. (5)}$$

where p, q, r is an equivalent body rates, or inputs to inner loop controller; α, β, ϕ refer to slow variables of outer loop; $N_z p$ is normal acceleration at pilot station; V is an air speed; θ refer as pitch attitude (rad); and V_{CO} is the crossover velocity. All these parameters have not be suitable for neither high rates of angle of launch and swoop nor slow velocity (*Figure 1*).

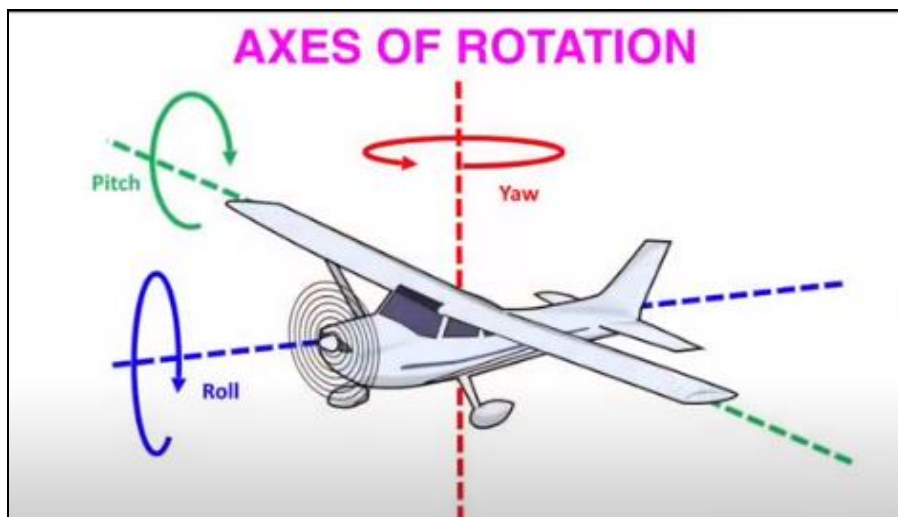


Figure 1. Axes of aircraft body rotation.

Dynamic inversion controller DI

To treat with the nonlinear properties of aircraft, there are many techniques that take advantage of the nonlinearity of the controller in order to improve the performance of the system. A dynamic inversion is one of these techniques. This technique requires knowledge of the nonlinear aircraft model, and this requires high-powered computers. As known in square control systems particularly, the tracked and controlled output $y(t)$ must follow the desired reference $r(t)$. According to the dynamic inversion technique, the output of the system $y(t)$ is derived until the controlling signal $u(t)$ will found in the derivation equation. This is the input/output feedback for linearization. Taking the first derivative results in:

$$y' = (Cx)' = CAx + Cbu \quad \text{Eq. (6)}$$

$$v = Ke \quad \text{Eq. (7)}$$

$$\dot{e} = -Ke \quad \text{Eq. (8)}$$

Eq. (7) represents an outer feedback as proportional tracking loop. While Eq. (8) represents the closed-loop for error dynamics. The gain values should be positive and diagonal to achieve aircraft stability and achieve flying requirements. The gain K values

must be chosen to suit the requirements of the flight. As shown in *Figure 2*, the total input of dynamic inversion controller as in Eq (9).

$$u = (CB)^{-1} (\dot{r} + Ke - CAx) \quad \text{Eq. (9)}$$

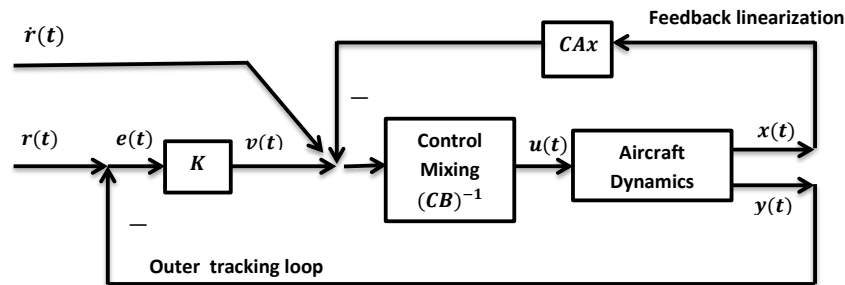


Figure 2. Dynamic inversion controller DI.

Feedback linearization is an inner control which use full state variable. The importance of this circuit lies in making the system appear linear. It is make the system between $v(t)$ to $y(t)$ look like a linear system with origin poles. Hence, this will lead to simple outer tracking loop design. The function of in *Figure 2* is to improve the tracking of closed loop. MATLAB software has used to simulate this controller. To represent the nonlinear properties of the aircraft model dynamics, the very important MATLAB M_file has required. The DI controller has designed as indicated in Eq. (9) first, which is the part that represents the real code of the aircraft controller. After that, state equations derivatives are calculated for the aircraft model. As mentioned earlier, it is important to know the dynamics of the plane by the controller represented by the input and output matrices of the system. The $r(t)$ desired trajectory has chosen as a unity step form. If the aircraft step response close enough to the shape of the input signal, then the controller considered acceptable and for a pilot's orders upon entry.

Nonlinear dynamic inversion controller NDI

As mentioned previously in this paper, the designed controller has divided into two parts, one of them uses Nonlinear dynamic inversion NDI and the other is Dynamic inversion DI. That is, the system has used two external and internal loops for this purpose. The external loop commands have generated by a special algorithm, and these commands have also converted into equivalent body rates (p, q, r). These rates will be the input to the controller for the internal loop. Whereas the internal loop will produce the required deflection commands at each entry profile coming from the external loop. This deflection will push the mission to the model plant (Laxman et al., 2020). A longitudinal model of an aircraft (*Figure 3*):

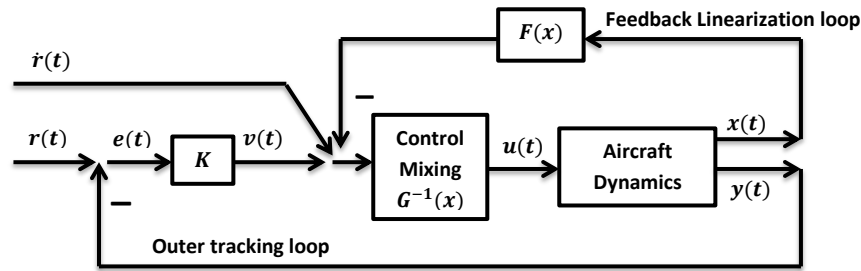


Figure 3. Nonlinear dynamic inversion controller NDI.

$$\dot{x} = f(x) + g(x)u \quad \text{Eq. (10)}$$

The states variables are:

$$x = [v_T \ \alpha \ \theta \ q \ \delta]^T \quad \text{Eq. (11)}$$

v_T =true air speed (rad/second), α =angle of thrust (rad), θ =pitch attitude (rad), q =pitch rate (rad/second), and δ =elevator actuator= $\theta - \alpha$. It is noticeable that when the value of $\theta = \alpha$, then $\delta = 0$ for level flight, and $q = 0$ for steady state, as well as u is the elevator actuator input. The normal acceleration at the center of gravity of the aircraft is given by Eq. (12).

$$N_z = \bar{q}S(C_L \cos \alpha + C_D \sin \alpha)/mg \quad \text{Eq. (12)}$$

C_L : Linear lift curve representation, and C_D : Parabolic drag. The normal acceleration at the pilot's station is given by Eq. (13).

$$N_{zp} = N_z + 15 \dot{q}/g = \bar{q}S(C_L \cos \alpha + C_D \sin \alpha)/mg + 15M/gI_{yy} \quad \text{Eq. (13)}$$

It can assumed that the model system has be square, so, the number m of inputs will be equal to the number p of outputs. This lead to vectors $u(t)$ and $y(t)$ will have identical dimension moment of inertia, m is mass=weight/ g , where g : gravitational constant. Added pitch damping M represents the pitching moment (MOM). The output is selected as:

$$y = C^* = N_{zp} + 12.4q \equiv h(x) \quad \text{Eq. (14)}$$

The states are r is yaw rate, β is sideslip angle, p is roll rate, ϕ is bank angle, δ is actuator states, and S is wing reference area. From Figure 3, the overall dynamic inversion controller is given by:

$$u = G^{-1}(x) [-F(x) + \dot{r} + Ke] \quad \text{Eq. (15)}$$

So the aim is to apply Eq. (15) to determine the dynamic inversion controller. So, one should find $F(x)$ and $G(x)$:

$$F(x) = \frac{\partial h}{\partial x} f(x) \quad \text{and} \quad G(x) = \frac{\partial h}{\partial x} g(x) \quad \text{Eq. (16)}$$

Finally, one has:

$$\frac{\partial C^*}{\partial x} = \frac{\partial n_z}{\partial x} + \frac{15}{gI_{yy}} \frac{\partial M}{\partial x} + k \quad \text{Eq. (17)}$$

The gain k must be chosen in order the zero dynamics will be stable. The determination of matrices of controller has used MATLAB simulation consisting of both controller and aircraft dynamics model. It is clear that the *Figure 3* contains a dynamic model of the aircraft and for this it has required $F(x)$ and $G(x)$. The Eq. (18) represents the *Figure 3* where it is shown that the nonlinear attributes are converted to linear to enable easy handling.

$$\dot{x} = f(x) + g(x) G^{-1}(x) [-F(x) + \dot{r} + v] \quad \text{Eq. (18)}$$

Results and Discussion

Simulation

The performance verification of this controller has employed by MATLAB toolbox as simulation systems. The effect of proportional controller gain will be explained in this section. It is important to review the definition of some variables used in simulation of the aircraft dynamics model: weight=2300 (lbs), $g=32$ (ft/s²), $I_{yy}=2000$ (slug ft²), $S=175$ (ft²).

Simulation of uncontrolled aircraft at proportional linear gain $K=10$

Figure 4 represents the simulation of state variables as in Eq. (11). These results for uncontrolled aircraft which will retain their values when the controller is applied to the aircraft model as shown next results.

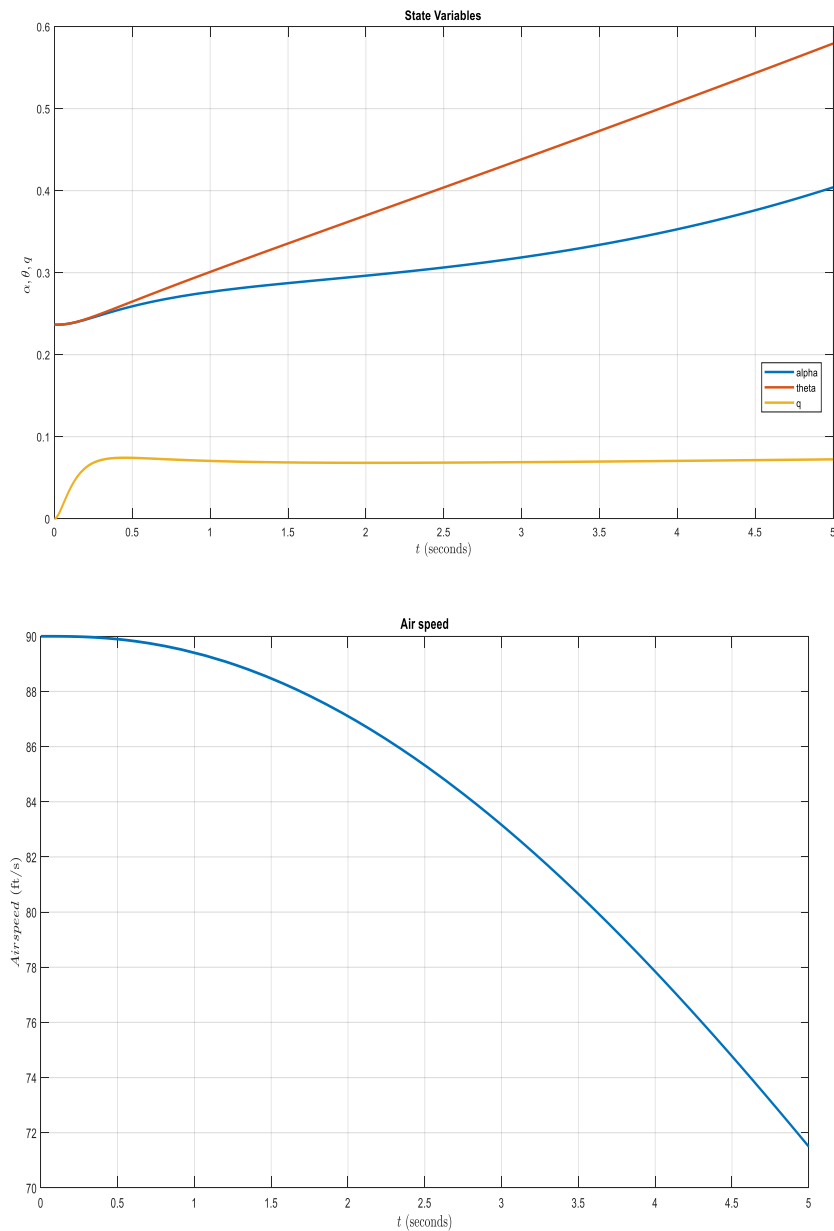


Figure 4. Simulation of aircraft state variables: a- α (rad), θ (rad), q (rad/second);
 b- v_T (rad/second).

Simulation of controlled aircraft at proportional linear gain $K=10$

Figure 5 represents the angle of thrust in rad with respect to time, which increases from 0.24 to 0.4 within 5 seconds. Figure 6 represents the fifth column of Eq. (11), which is the elevation angle that decreases sharply in the reverse direction at the beginning of time, and then gradually increases until it enters the stabilization phase after only 1.5 seconds.

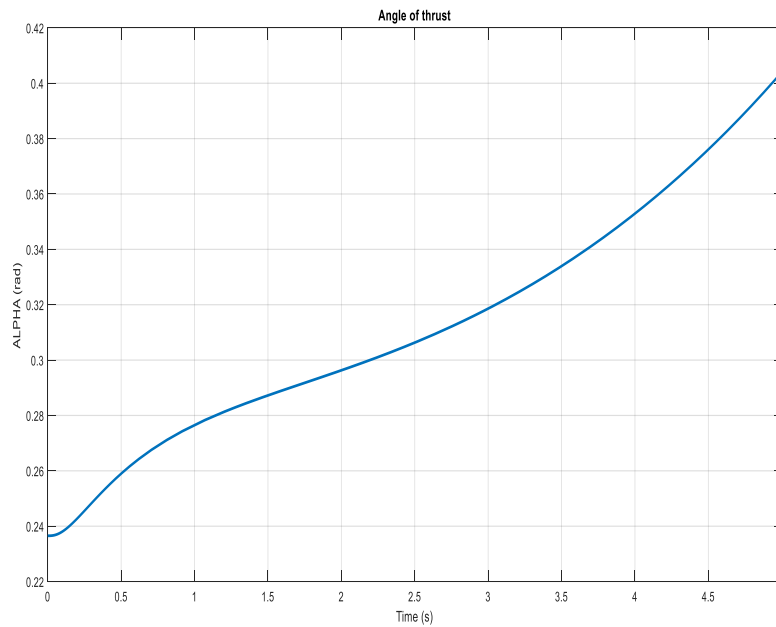


Figure 5. Angle of thrust (rad) with time at $K=10$.

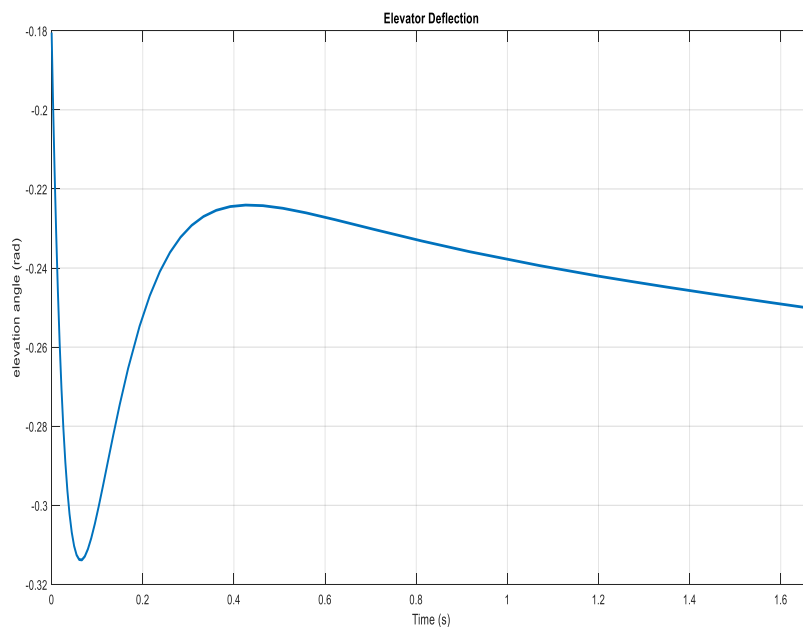


Figure 6. Elevator deflection (rad) with time at $K=10$.

Figure 7 represents theta angle, which is the angle of ascent of the aircraft during 5 seconds, as it ascends at about 0.24 rad. This is a stable linear increasing, and this is desirable in controlling of aircraft. *Figure 8* represents the output of the control system. It shows the dynamic response to the movement of the aircraft in harmony with the required input commands, which are directed to both the aircraft and the controller system. Note that the input has been selected as the unit step function. It turns out that the output reaches the steady state after 0.4 seconds, and this is called the delay time. It

is obvious from the curve that no overshoot or distortion appears, and this is what discriminate the design here as will be shown later in this section.

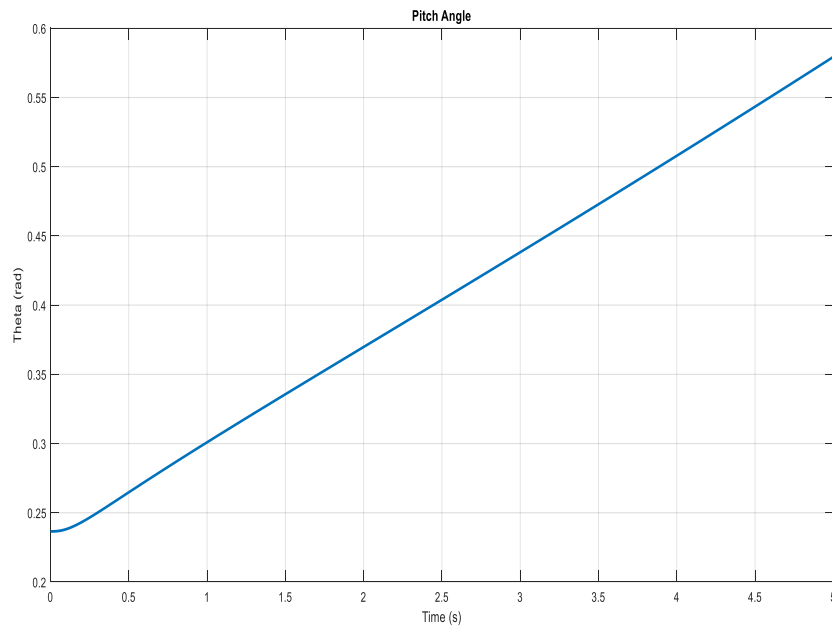


Figure 7. Pitch angle (rad) with time at $K=10$.

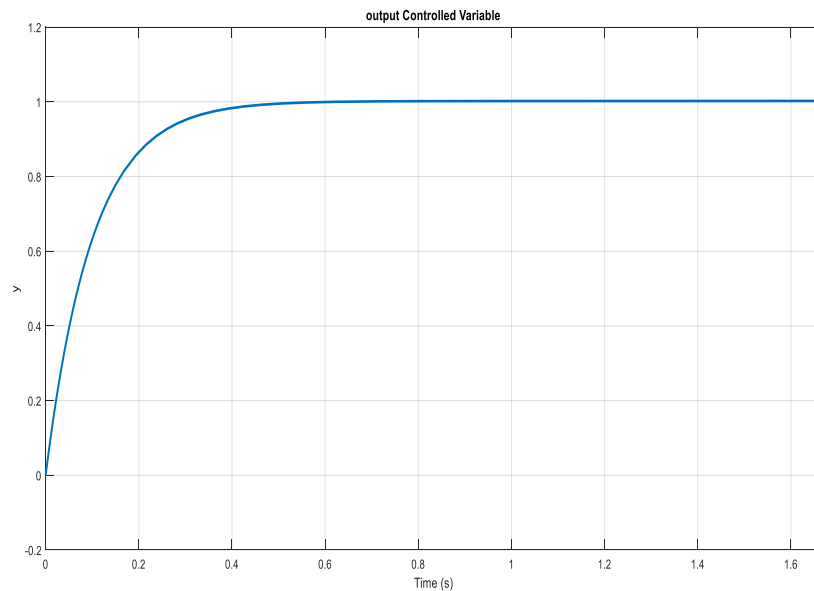


Figure 8. Output Controlled Variable (Y) with time at $K=10$.

The pitch rate of the aircraft has shown in *Figure 9*. The time of the aircraft flight stability is approximately 1.6 seconds, so its ascent remains balanced at 0.07 rad/s. This figure shows that the aircraft ascent angular rate increases at the beginning to reach the highest rate of approximately 0.075 rad/s and this is considered an acceptable pitch rate. Pitch rate or the variable 'q' is the fourth column in the aircraft state matrix as in Eq. (11). The *Figure 10* represents the heights reached by the aircraft in this design,

according to the aforementioned equations. As for *Figure 11*, it represents the DRAG of the aircraft, which depends on the quantities shown above and according to the aforementioned equations. *Figure 12* represents how the pitch will dampen 'MOM' during the ascent movement of the aircraft, which is concentrated at the beginning of the movement. This pitch damping has been at the first 500 seconds, where the damping peak reaches 900/rad and then falls back to zero and stabilizes at that value.

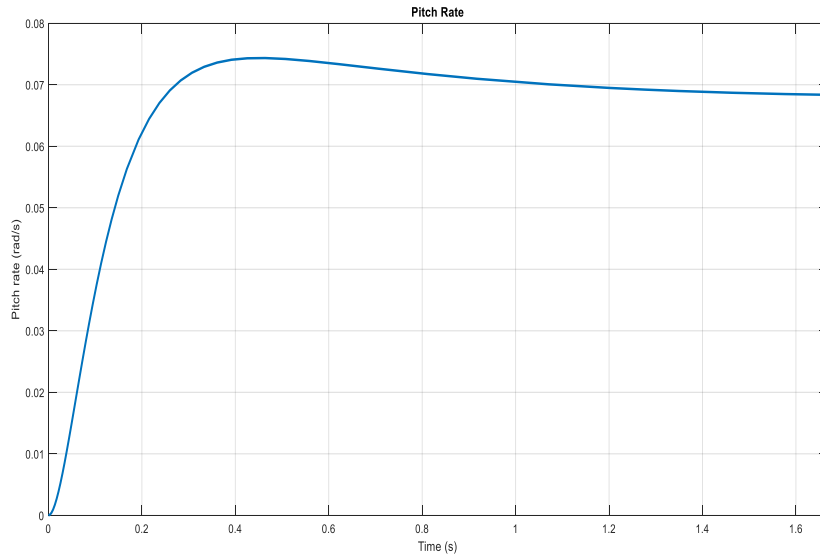


Figure 9. Pitch rate (rad) with time at $K=10$.

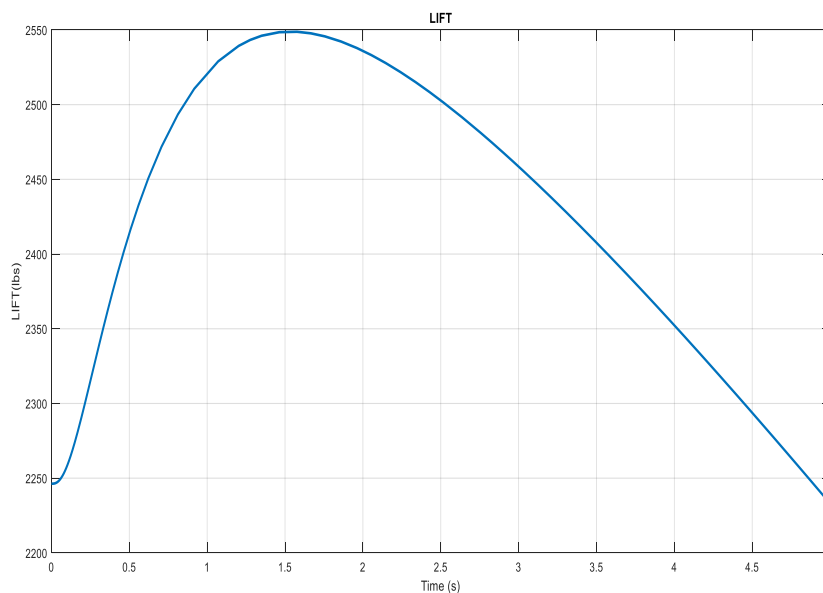


Figure 10. Aircraft heights simulation (lbs) with time at $K=10$.

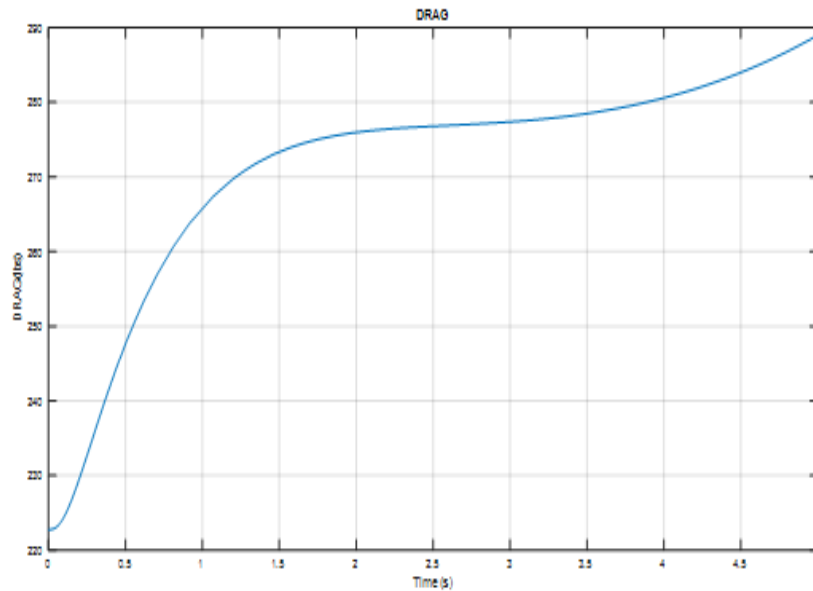


Figure 11. Aircraft drag simulation (lbs) with time at $K=10$.

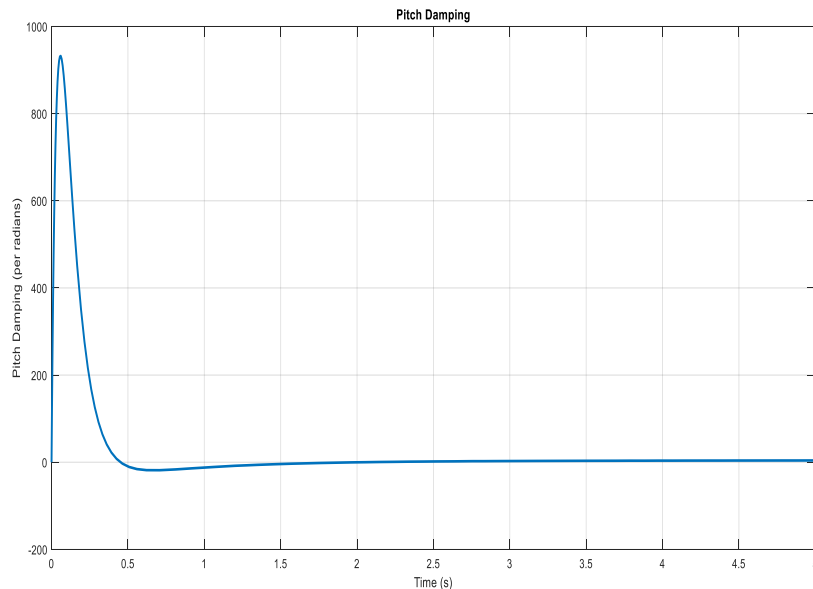


Figure 12. Aircraft pitch damping (/rad) with Time at $K=10$.

Figure 13 represents one of the outputs of the controlled model, which is the normal acceleration at the center of gravity of the aircraft. It increases to reach its peak of 0.155 at approximately one second and then gradually decreases till stable movement of the aircraft. The normal acceleration has represented at another location of the aircraft to further clarify the dynamic stability of the aircraft during its ascent. Figure 14 represents the normal acceleration at the location of the pilot's station, which alternates in the period up to two seconds and then the curve tends to stability to reach $N_{zp}=0.11$.

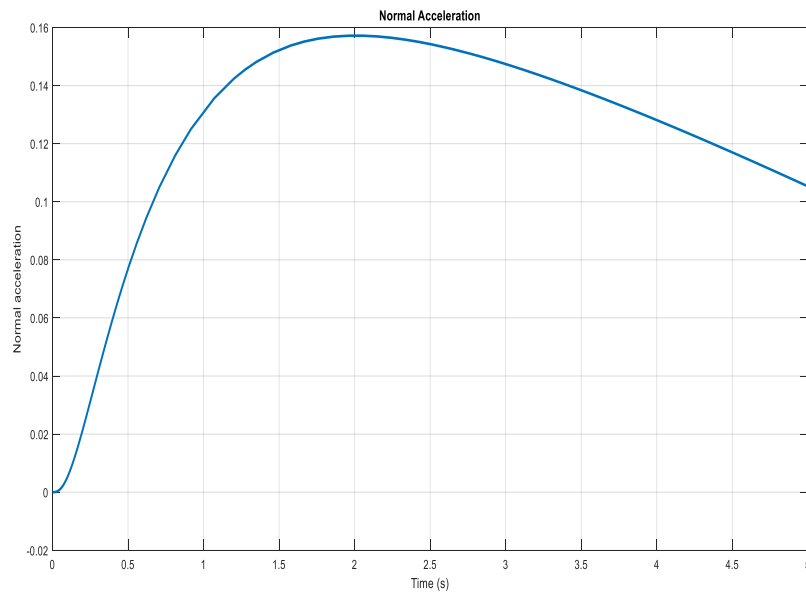


Figure 13. Normal acceleration at the center of gravity of the aircraft at $K=10$.

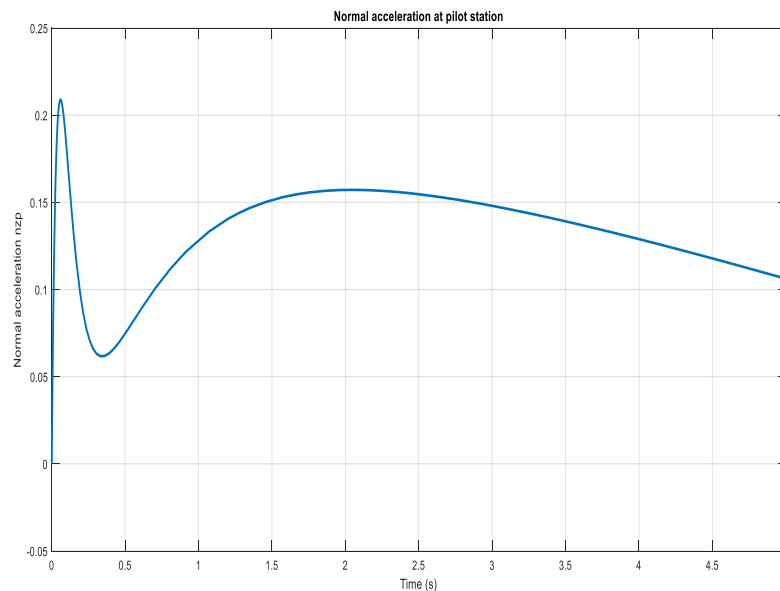


Figure 14. Normal acceleration at the pilot station of the aircraft at $K=10$.

Effect of proportional controller on the dynamic stability of aircraft

In this section, the effect of proportional controller gain is clarified. After all presented results of controlled aircraft model which considered gain $K=10$, the results would be altered when $K=20$. So, the next figures will explain the case of increasing gain of those differ results only. This means that results have appeared same as first case will not be presented here to avoid recurrent results. It is obvious from *Figure 15* here a sharp decrease in the elevator deflection angle of -0.38 which is less than elevation angle at the gain of 10. The curve enters the stabilization state at a time less than it was in the previous case of gain. The output here in *Figure 16* is very close to the

input form, and this is the preferred one, and it reaches the steady state at 0.25 seconds, which is less time than it was in the previous case (0.5 seconds), and this shows the advantages of increasing gain here particularly.

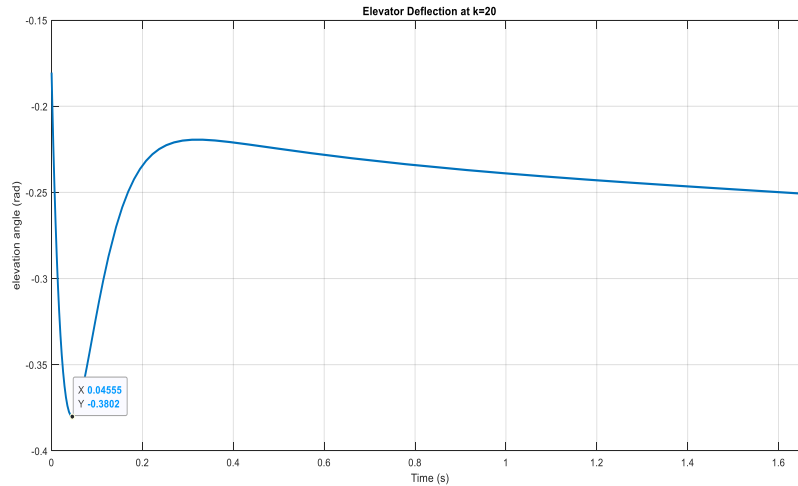


Figure 15. Elevator Deflection (rad) with Time at $K=20$.

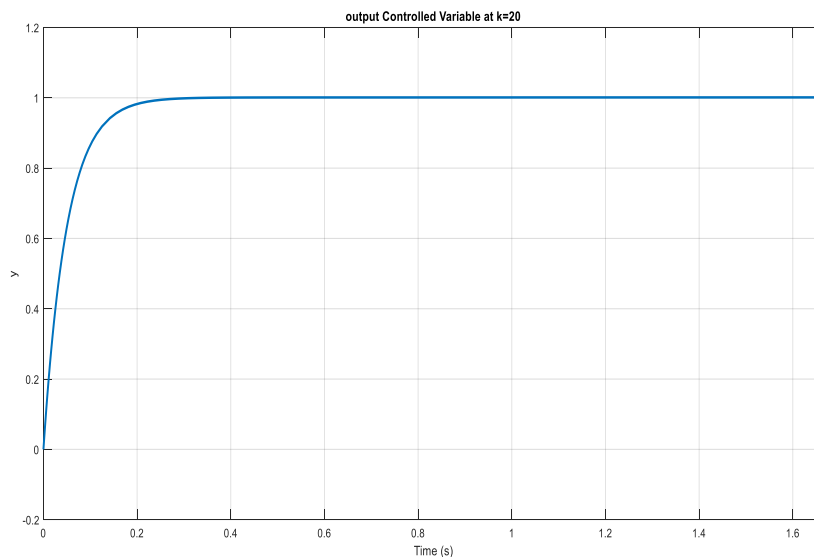


Figure 16. Output Controlled Variable (Y) with Time at $K=20$.

In pitch rate result as *Figure 17*, the highest value reaches at a faster time of 0.28 seconds and then enters the steady state at a faster time than in the previous gain. A clear difference is in the greatest value reached by the pitch damping (*Figure 18*). This value increases significantly when increasing the gain, but on the other hand, stability could be at a time less than that in the previous case of the gain. It is noticed from *Figure 19* that the acceleration peak increased to reach 0.32 compared to the previous case of the gain, which had reached 0.21. The stability of acceleration will be at 0.11 as well as before.

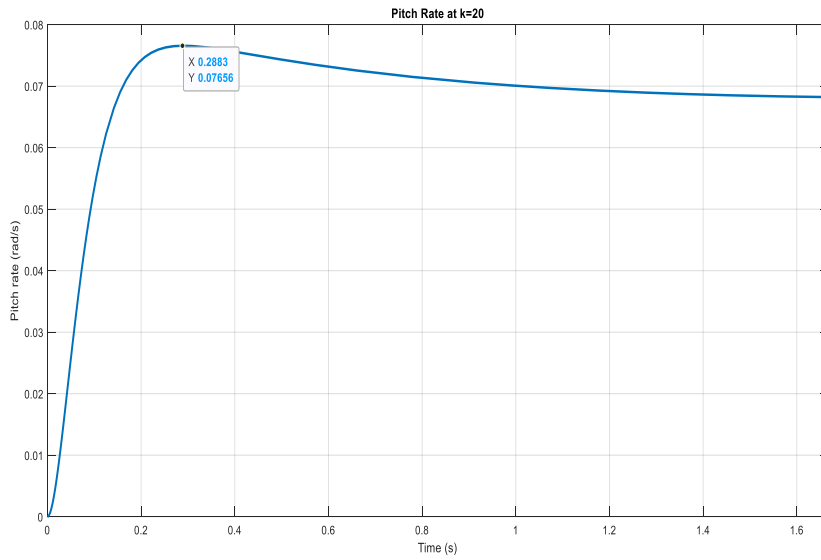


Figure 17. Pitch rate (rad) with time at $K=20$.

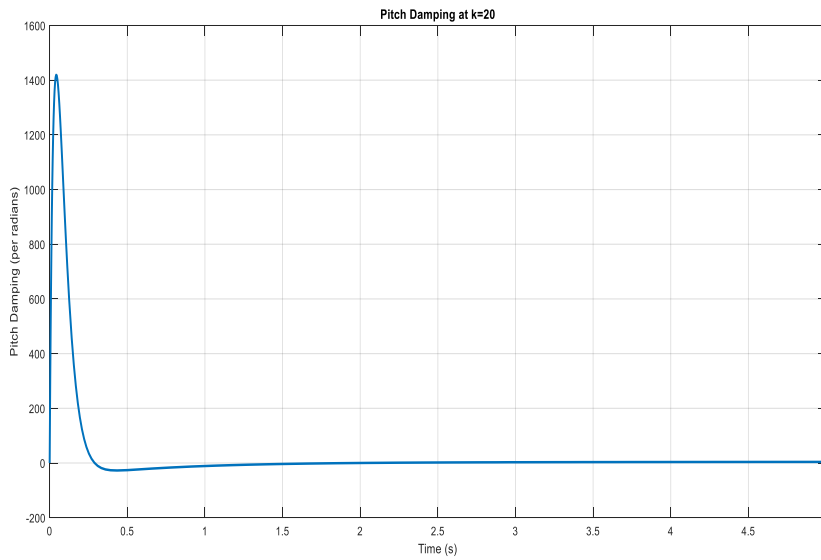


Figure 18. Aircraft pitch damping (/rad) with time at $K=20$.

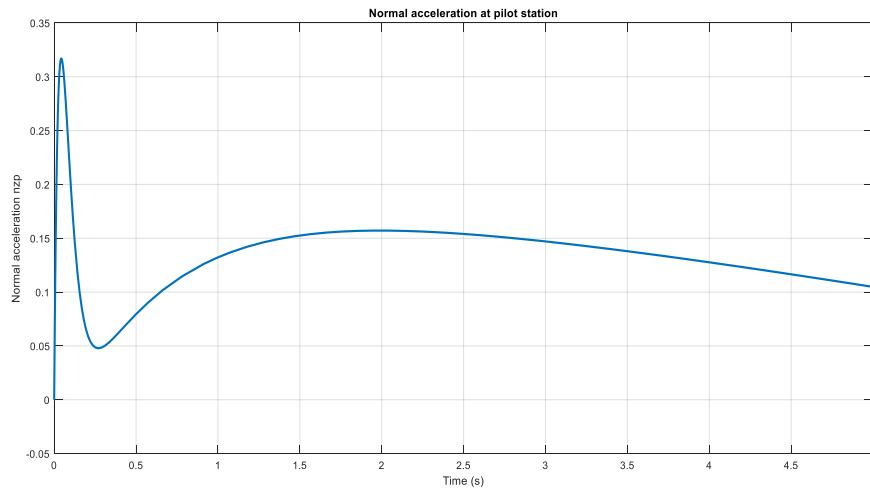


Figure 19. Normal acceleration at the pilot station of the aircraft at $K=20$.

The dynamic stability of aircraft model without proportional controller

Figure 20 and Figure 21 have shown the instability of the movement of the aircraft during its ascent, and this is caused by the absence of the proportional controller. Hence, it is evident the great influence of the proportional controller on all the results.

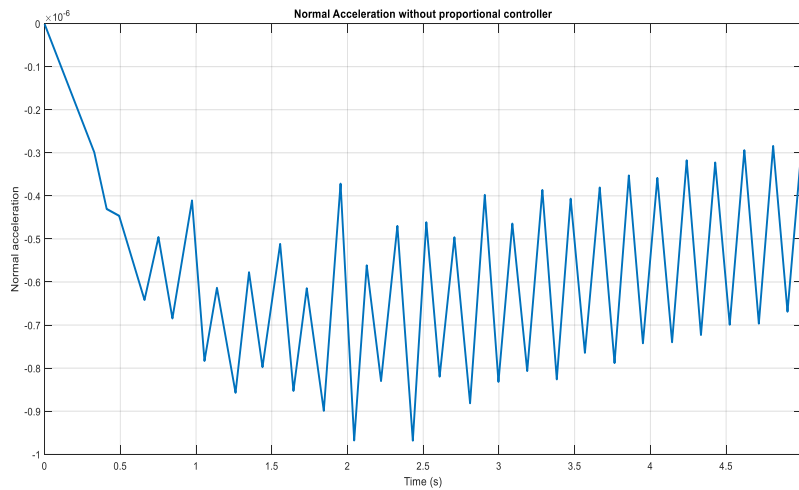


Figure 20. Normal acceleration at center of gravity of the Aircraft at $K=0$.

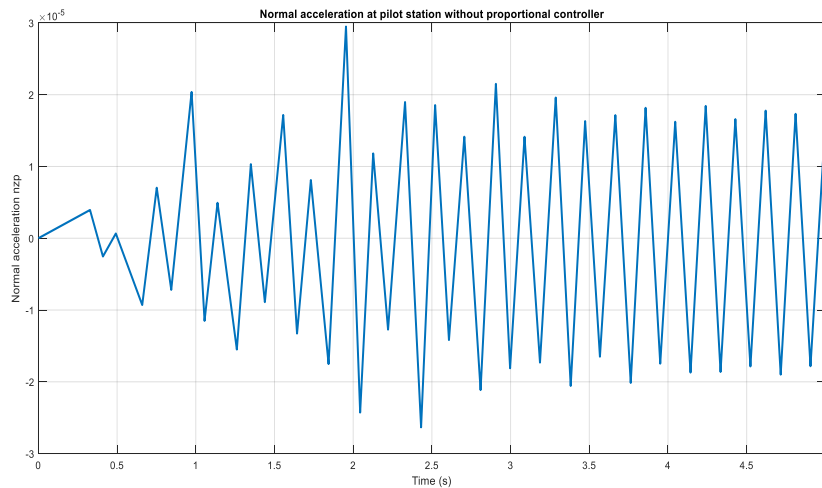


Figure 21. Normal acceleration at pilot station of the aircraft at $K=0$.

Conclusion

This work has resulted in effect and importance of existence the proportional controller with nonlinear dynamic inversion controller on the aircraft dynamic model. The aim of design controller is to achieve a best response in output based on the input command. This exactly presented in the output controlled variable especially when increase the gain of proportional controller in the outer loop of aircraft control system. The results have shown when increasing the gain , the time needed to enter steady state and stability dynamics will be less. On the other hand, the amplitude of un-stability and curve distortion in the beginning dynamics curve will be stronger as gain increased. There is a need of tradeoff between two cases to get reasonable performance of aircraft control model.

Acknowledgement

After completing this work, I would like to express my heartfelt thanks to everyone who encouraged me and gave me advice and guidance in achieving the goal, hoping that the benefit of this research will prevail.

Conflict of interest

The author declares no conflict of interest, financial or otherwise.

REFERENCES

- [1] Almalah, N.T., Al-Tayyar, H.A. (2020): Development of a Longitudinal Control Model of an Aircraft with Gusty Environment. – International Journal of Computer Applications 176(38): 29-33.
- [2] Al-Tayyar, H.A., Almalah, N.T. (2020): Aircraft animation and air route tracing simulation system. – In AIP Conference Proceedings, AIP Publishing LLC 2213(1): 6p.

- [3] Bhardwaj, P., Akkinapalli, V.S., Zhang, J., Saboo, S., Holzapfel, F. (2019): Adaptive augmentation of incremental nonlinear dynamic inversion controller for an extended f-16 model. – In AIAA Scitech 2019 Forum 21p.
- [4] Di Francesco, G., Mattei, M. (2016): Modeling and incremental nonlinear dynamic inversion control of a novel unmanned tiltrotor. – Journal of Aircraft 53(1): 73-86.
- [5] Laxman, R., Maity, A., Mallikarjun Rao, G., Kranthi Kumar, R. (2020): Optimal nonlinear dynamic inversion-based flight control system design for an aerospace vehicle. – In Advances in Small Satellite Technologies, Springer, Singapore 21p.
- [6] Lombaerts, T., Kaneshige, J., Schuet, S., Aponso, B.L., Shish, K.H., Hardy, G. (2020): Dynamic inversion based full envelope flight control for an eVTOL vehicle using a unified framework. – In AIAA Scitech 2020 Forum 30p.
- [7] Lu, K., Liu, C. (2019): A L1 Adaptive Control Scheme for UAV Carrier Landing Using Nonlinear Dynamic Inversion. – International Journal of Aerospace Engineering 9p.
- [8] Matamoros, I., de Visser, C.C. (2018): Incremental nonlinear control allocation for a tailless aircraft with innovative control effectors. – In 2018 AIAA Guidance, Navigation, and Control Conference 25p.
- [9] Sieberling, S., Chu, Q.P., Mulder, J.A. (2010): Robust flight control using incremental nonlinear dynamic inversion and angular acceleration prediction. – Journal of Guidance, Control, and Dynamics 33(6): 1732-1742.
- [10] Smeur, E.J., de Croon, G.C., Chu, Q. (2018): Cascaded incremental nonlinear dynamic inversion for MAV disturbance rejection. – Control Engineering Practice 73: 79-90.
- [11] Stevens, B.L., Lewis, F.L., Johnson, E.N. (2015): Aircraft control and simulation: dynamics, controls design, and autonomous systems. – John Wiley & Sons 768p.
- [12] van't Veld, R., Van Kampen, E.J., Chu, Q.P. (2018): Stability and robustness analysis and improvements for incremental nonlinear dynamic inversion control. – In 2018 AIAA Guidance, Navigation, and Control Conference 17p.
- [13] Wang, X., Van Kampen, E.J., Chu, Q., Lu, P. (2019): Stability analysis for incremental nonlinear dynamic inversion control. – Journal of Guidance, Control, and Dynamics 42(5): 1116-1129.